Rezgui, D., Lowenberg, M. H., Jones, M., & Monteggia, C. (2014). Continuation and Bifurcation Analysis in Helicopter Aeroelastic Stability Problems. *Journal of Guidance, Control, and Dynamics*, *37*(3), 889-897. https://doi.org/10.2514/1.60193

Continuation and Bifurcation Analysis in Helicopter Aeroelastic Stability Problems

Djamel Rezgui[1] and Mark H. Lowenberg[2]
University of Bristol, Bristol, BS8 1TR, UK

Mark Jones[3]
AgustaWestland Ltd, Yeovil, Somerset, UK

Claudio Monteggia[4]
AgustaWestland SPA, Cascina Costa, Italy

The dynamics of rotary wing systems is complex and typically features highly nonlinear and often unsteady aerodynamics as well as aeroelastic influences. In ongoing efforts to reduce noise and vibration, active devices such as trailing edge flaps on the rotor blades are being studied and these devices can introduce further nonlinearities. Therefore, it is important to be able to evaluate the stability of the overall system with a proper understanding of the global nonlinear behavior. Numerical continuation and bifurcation analysis is well suited to this need, and this paper presents evidence of the technique providing a deeper insight into the stability of helicopter rotor systems than the methods typically adopted in industry. We first investigate the aeroelastic stability of rotor blades of a medium-sized helicopter in hover and the periodically forced forward flight condition, in both trimmed and untrimmed cases. Then, bifurcation analysis is used to predict the nonlinear stability of a single degree-of-freedom trailing edge flap added to the aeroelastic system, over a range of design parameters. The approach is novel in the context of real-world aeroelastic rotor models, and the

---

[1] Lecturer in Rotorcraft Technologies, Dept. of Aerospace Engineering, University of Bristol, UK, and AIAA Associate Member.
[2] Reader in Flight Dynamics, Dept. of Aerospace Engineering, University of Bristol, UK, and AIAA Senior Member.
[3] Senior Engineer, Rotor Dynamics and Loads, Helicopter System Design, AgustaWestland Ltd, Yeovil, Somerset, UK.
[4] Manager, Rotor Dynamics and Loads, Helicopter System Design, AgustaWestland SPA, Cascina Costa, Italy.

emphasis here is on the potential for revealing important multiple-attractor dynamics rather than the study of a particular system. The results presented highlight the advantages of the approach, both in terms of generating an understanding of local and more global stability, and in the efficiency in obtaining relevant results as parameters vary.

Nomenclature

$(\,)'$	= Differentiation with azimuth angle ψ.
$\dot{(\,)}$	= Differentiation with time t.
A_{lat}, B_{long}	= Lateral and longitudinal cyclic pitch angles.
I_i	= Modal mass of mode i.
L, D	= Elemental aerodynamic flapwise and lagwise force components, positive upward and forward respectively.
L_0, D_0	= Elemental aerodynamic flapwise and lagwise force components computed when the blade's modes are evaluated, positive upward and backward respectively.
M	= Elemental aerodynamic pitching moment about the section shear center, positive nose up.
M_0	= Elemental aerodynamic pitching moment computed when the blade's modes are evaluated, positive nose up.
N_B	= Number of blades.
Q_{q_i}	= Generalized force of mode i.
R	= Rotor radius.
T	= Rotor oscillation period.
T_i, T_{av}	= Rotor instantaneous and average thrust.
T_{req}	= Required rotor thrust.
U_P, U_T	= Perpendicular and tangential components of the elemental flow velocity.
c_{tef}, k_{tef}	= Linear rotational damping and stiffness coefficients at the trailing edge flap hinge.
h_s, h_c	= Harmonic oscillator states, $h_s = \sin(\Omega t)$ and $h_c = \cos(\Omega t)$.
p	= Parameter vector describing the rotor and flow properties.
q_i	= Generalized displacement of mode i.

r = Elemental blade radial position.

t = Time.

u = Blade axial displacement.

w, v, φ = Blade flapwise, lagwise, and twist deflections respectively.

w_i, v_i, φ_i = Flapwise, lagwise and twist components of the i^{th} mode shape respectively.

$w_{st}, v_{st}, \varphi_{st}$ = Blade flapwise, lagwise and twist steady state deflections respectively.

x = State vector.

Ω = Rotor speed.

β = Blade flapping angle.

$\beta_{a_1,req}$, $\beta_{b_1,req}$ = Required lateral and longitudinal flapping angles respectively.

δ = Trailing Edge Flap (TEF) angle.

μ = Advance ratio.

ν_i = Induced velocity at blade radial position r and azimuth ψ.

ν_0, ν_s, ν_c = Average, lateral and longitudinal induced velocity components respectively.

ω_{q_i} = Modal frequency of mode i.

ϕ = Inflow angle.

ψ = Azimuth angle.

θ_{col} = Collective pitch angle.

θ_p = Pre-deformed blade pitch angle, $\theta_p = \theta_{pt} + \theta_{col} - A_{lat}\cos(\psi) - B_{long}\sin(\psi)$.

θ_{pt} = Blade pre-twist or built-in twist angle.

I. Introduction

The dynamics of rotary wing systems involve complex interactions of aerodynamic, structural, material and geometric nonlinearities. In the helicopter industry, the trend towards higher performance gains and lower vibration and noise levels has led to the development of more complex rotor systems, which incorporate novel design features, utilizing for example: composite materials, semi-active lag dampers and active trailing edge flaps. These features tend to increase the levels of nonlinearity in the rotor system, which means that a proper nonlinear analysis of the blade dynamics is required. Traditionally, different mathematical techniques have been used to study the aeromechanical and aeroelastic blade stability, at different flight regimes. These techniques

include time history simulation (time integration techniques), parametric resonance analyses [1–3], perturbation methods [4, 5] and Floquet analysis [5–7]. In fact, in most operating conditions, the helicopter blade aeromechanical and aeroelastic stability is well understood in both the academic and industrial sectors, including cases of very high tip speed ratios. Extensive reviews in the field are those by Friedmann and Hodges [8], and Friedmann [9].

However, many of the above stability methods depend on assumptions that are questionable for newer rotor configurations such as rotors with very flexible blades or with active/actuated elements, where highly nonlinear dynamics are introduced. In addition, these methods may not provide the complete stability picture. For example, the methods can predict the local stability of the blade, but the regions of attraction in that case are not defined. In other words, the blades might be stable for small disturbances but feasible disturbances may be large enough for the local stability to be lost and the actual outcome is not indicated. In nonlinear mathematics, the regions of attraction can be obtained by predicting the multiple-attractor structure governing the nonlinear dynamics of a system in the larger state space. This structure portrays the main as well as secondary solutions, both stable and unstable, which can give an indication of how large the perturbations would need to be for the dynamical system to change its behavior from that predicted by local stability analysis. Therefore, it can be inferred that, unlike local linearized methods, nonlinear stability methods can not only indicate the dependence of system stability on parameter variation, including boundaries in parameter space between stable and unstable conditions, but they also provide more global information on likely behavior via the solution of multiple attractors and their influence on dynamic response. One of these powerful nonlinear analyses is dynamical system theory, implemented in the form of bifurcation and continuation methods. The benefits of these methods over those mentioned above lies not only in gaining a more global picture of the system dynamics through the computation of multiple solution branches, but also in the efficiency in obtaining these solutions with their stability and identifying the types of bifurcation, which indicate changes in the dynamics [10].

In the aerospace sector, the use of bifurcation and continuation tools is becoming more widespread. In particular, it is increasingly adopted to investigate nonlinear aircraft flight dynamics and control problems. However, the application of continuation and bifurcation methods has been limited to a small number of helicopter dynamical problems, such as flight mechanics [11–17], ground resonance [18, 19] and examination of rotor vortex ring state [20]. Furthermore, almost all of the investigations which utilize these nonlinear tools can be regarded as research studies and it is still hard to find these tools adopted in industry for production aircraft. In recent years, the stability of rotor blades in autorotation was investigated by Rezgui *et al.* [21, 22] and Lowenberg *et al.* [23] using nonlinear dynamics theory implemented numerically in the form of continuation and bifurcation methods. The same techniques were also adopted by Rezgui *et al.* [24] to investigate the aeroelastic rotor blade stability of helicopter rotor blades. This investigation showed that these techniques are powerful in the identification of instability scenarios of rotor blades and uncovering the multiple solution structure driven by the nonlinearities in the rotor system. However, this work focused mainly on the applicability of the methods to helicopter blade stability problems without fully discussing the effects and importance of nonlinearities on the global dynamics and hence the global stability of the rotating aeroelastic blade.

The inclusion of complex active or even passive dynamic systems in a rotating blade may introduce further nonlinearities, which can introduce undesirable behavior within the operating range and physical design space. One of these devices is the Trailing Edge Flap (TEF), which has been considered by helicopter manufacturers for vibration reduction, noise reduction and performance gains. For example, the experimental BK117 was the first worldwide flying helicopter with an active rotor TEF system [25]. TEFs can be intelligently actuated and controlled in a closed-loop fashion to locally change the aerodynamic lift and moment distributions on the blades, and thus, obtain the desired gains. Furthermore, due to the presence of TEF dynamics the blade motion can be significantly affected by the couplings between the blade degrees-of-freedom [26]. There are a number of studies that investigated the stability of TEFs incorporated in a rotor system such as the work by Shen and Chopra [27] and Maurice *et al.* [28]. However, these studies

investigated only the local linearized stability - using small perturbation motions about steady trimmed solutions - using the Floquet method and the nonlinear stability aspects were not studied. In a previous work, Straub and Charles [29] studied the coupled blade/flap dynamics using the comprehensive helicopter code CAMRAD II and showed that the TEF spring stiffness affects the stability of flap-pitch and fundamental blade torsion modes. Again this analysis was based on eigen-analysis and the global nonlinear aspects of the coupled blade/flap dynamics were not investigated. Therefore, it is still not clear if nonlinearities inherent in the TEF system or those already inherent in the rotor system can lead to undesirable behavior of the coupled TEF/blade system. Other examples of sources of nonlinearity in the rotor system include nonlinear damping properties of passive or semi-active lag dampers, hardening effects of pitch-link mechanisms and free-play in the swash-plate system.

This paper shows, for the first time, possible stability scenarios for a trailing edge flap on an aeroelastic rotor, which are driven by the inherent nonlinearities in the coupled TEF/blade system. The approach is suitable for both low-order and more complex models. Relevant concepts in continuation and bifurcation analysis are described in sec. II. Then in sec. III, the aeroelastic model is introduced and its nonlinear behavior examined using bifurcation analysis. The trailing edge flap is introduced to the model in sec. IV and the resulting nonlinear characteristics explained. Conclusions on the benefits and applicability of the methods are drawn in sec. V.

II. Continuation and Bifurcation Methods for Rotorcraft Applications

The basic idea of the numerical continuation and bifurcation techniques is the calculation of the steady solutions of a dynamical system as one of its parameters, called the continuation parameter, is varied across a pre-defined range. The computed solutions construct a number of branches that could be either stable or unstable. To determine the stability, either an eigen or Floquet analysis is carried out at each computed solution, depending on the nature of the solution. For instance, in hover the blade behavior can be considered to be in equilibrium (fixed points), hence an eigen analysis is carried out for stability, whereas in forward flight, the blades behave in a periodic manner

(limit cycles) due to the rotor lift asymmetry, hence Floquet theory is used to determine the stability.

A bifurcation is the qualitative change in the system behavior as a parameter is varied. In other words, when the stability of a system is changed or lost, the system bifurcates. The points at which these stability changes happen are called bifurcation points. When the system is nonlinear, new solution branches may emerge from the bifurcation points, leading to the presence of multiple solutions for the same set of system parameters. The identification of these different solution branches helps to uncover the global dynamics of the system. Of particular interest is when the blades, for example, are locally stable for small disturbances but not necessarily for large ones, and vice-versa.

Therefore, the strategy in implementing continuation and bifurcation methods is to follow one solution branch as one or more parameters are varied to locate bifurcation points. The emerging branches are then followed to construct a more complete picture of the system dynamics (bifurcation diagram). Furthermore, other advantages of continuation methods are their efficiency and accuracy in following the solution branches as well as in detecting and identifying the bifurcation points, compared with other time history or frequency domain methods. The different types of bifurcations that can occur in equilibria or periodic orbits are not discussed in this paper; the reader is referred to general texts such as references [10] for more background on the subject.

The continuation algorithm used in this analysis is implemented in the continuation and bifurcation software AUTO [30]. AUTO is open source software for continuation and bifurcation problems of ordinary differential equations, originally developed by Eusebius Doedel, with subsequent major contributions by several people[1] where it is currently available on a number of platforms [30, 31]. Besides many other types of equations, AUTO can perform extensive bifurcation analysis of ordinary

[1] The software can be downloaded from `http://indy.cs.concordia.ca/auto`

differential equations (ODEs) of the form:

$$\dot{x}(t) = f(x(t), p), \qquad x \in \Re^n, p \in \Re^m, f : \Re^n \times \Re^m \longrightarrow \Re^n \tag{1}$$

subject to initial conditions, boundary conditions, and integral constraints. Here x is the state vector and p denotes one or more parameters. n and m are the numbers of states and parameters respectively. Equation (1) is written in the generic (nonlinear) state-space form, where the state-derivatives are functions of the states and some parameters. One advantage of this form is the ability of passing the model variables to and from the analysis tool regardless of the environment where the system equations are coded (implementation procedures must be observed). This attribute provides a stability tool which not only is independent of the model but also is able to couple with a wide range of modeling platforms, which can be particularly beneficial in the helicopter industry.

The main two types of steady solutions which describe the rotor blade behavior in the conventional operating envelope are equilibrium and limit cycle solutions. Conventionally, helicopter rotor models are written in the non-autonomous form, in that the independent variable t (or ψ) appears explicitly in the equations. Of course in the hover case, the blade is in equilibrium and hence the model does not explicitly depend on the time variable t (or ψ), even if they appear in the standard equations. Therefore, for convenience the time variable t (or ψ) can be fixed to a constant value without affecting the model dynamics. On the other hand, in forward flight, the blade dynamics is heavily dependent on the blade azimuthal location, mainly because of the periodic aerodynamic forcing. In this case, the independent variable t (or ψ) has to be converted to a state variable. Of course, one can always designate the time t or azimuth angle ψ as additional states, in order to transform the system to an autonomous one. This can either be achieved by $\dot{\psi} = \Omega$, where ψ is a state or by $\dot{t} = 1$, where t is a state and the azimuth angle can be calculated as $\psi = \Omega\ t$, assuming Ω is constant. However, if the above method is used (either case), the new time state will monotonically increase and hence will not describe oscillatory behavior. Therefore, to solve this problem, a harmonic oscillator model is used to realize the periodicity of all states. The harmonic

oscillator equations are:

$$\begin{aligned} \dot{h_s} &= \quad h_s \quad + \Omega\, h_c \; - \; h_s\,(h_s^2 + h_c^2) \\ \dot{h_c} &= -\Omega\, h_s \; + \quad h_c \quad - \; h_c\,(h_s^2 + h_c^2) \end{aligned} \tag{2}$$

or

$$\begin{aligned} h_s' &= \quad h_s \quad + \; h_c \; - \; h_s\,(h_s^2 + h_c^2) \\ h_c' &= -h_s \; + \; h_c \; - \; h_c\,(h_s^2 + h_c^2) \end{aligned} \tag{3}$$

where the $h_s = \sin(\Omega\ t) = \sin(\psi)$ and $h_c = \cos(\Omega\ t) = \cos(\psi)$ are solutions to Equations (2) and (3). The terms h_s and h_c can now be used to replace any $\sin(\Omega\ t)$, $\sin(\psi)$, $\cos(\Omega\ t)$ or $\cos(\psi)$ in the blade forcing equations as appropriate. The azimuth angle can be calculated using the quadrant-arctangent function $\psi = \text{atan2}(h_s, h_c)$. This approach to the study of aeroelastic rotor blade dynamics has not previously been attempted, according to the literature.

III. Aeroelastic Stability of Helicopter Rotor Blades

A. Rotor Blade Model

In this section, the use of continuation and bifurcation analysis is illustrated in predicting the stability of helicopter main rotor blades in hover and forward flight conditions. The objective of this study is to determine how the inherent nonlinearities in a rotating aeroelastic blade manifest themselves in terms of adverse blade behavior. The nonlinearities included in the mathematical model were kept to the minimum and include geometric, inertial and structural terms arising from the formulation of the modal equations of a rotating blade, aerodynamics loads including static stall effect but excluding dynamic stall, and terms arising from coupling with the inflow model. Although dynamic stall is the primary source of nonlinearity, it was not modeled here to focus on the analysis of the effects of the other sources. We note, however, that state-space representations of unsteady aerodynamics such as dynamics stall (e.g. Leishman and Beddoes [32], Goman and Khrabrov [33]) are straightforward to incorporate within continuation and bifurcation analysis.

Modal representation is used for the structural blade dynamics and hence each blade is represented by a number of general modes (eight in this analysis: four flap, two lag and two torsional modes). The mode shapes, frequencies, and modal masses are computed a priori at a

given hover case condition. The computed modal characteristics are assumed to remain unaffected by the changes in flight condition. Although the model can include the dynamical equations for all blades of the rotor, it is adequate here to use a single bladed rotor model for the stability analysis.

The forced response equation approach is used to describe the aeroelastic dynamics of the blade. The equations used were developed in reference [34]. Figure 1 depicts a schematic drawing of the blade coordinate system and deflections v, w and φ, which can be calculated at each blade radial position r as follows:

$$w(r,t) = \sum_{i=1}^{n} q_i(t) w_i(r) + w_{st}, \qquad v(r,t) = \sum_{i=1}^{n} q_i(t) v_i(r) + v_{st}, \qquad \varphi(r,t) = \sum_{i=1}^{n} q_i(t) \varphi_i(r) + \varphi_{st} \quad (4)$$

where w_i, v_i and φ_i are the flapwise, lagwise and twist components of the i^{th} mode shape respectively. n is the number of modes and q_i is the generalized displacement. w_{st}, v_{st} and φ_{st} are the blade flapwise, lagwise and twist steady state deflections respectively. The formulation of this equation was done in a manner such that the orthogonality of the modes leads to an equation in which the modal response depends only on the following forcing components:

1. the aerodynamic forcing (Q_{aero,q_i});
2. time dependent terms such as the Coriolis force (Q_{tdep,q_i});
3. blade pitch dependent terms (Q_{pper,q_i});
4. nonlinear terms not included in the formulation of the modal equation (Q_{nlin,q_i}).

The forced response equation for each mode is:

$$\ddot{q}_i = -\omega_{q_i}^2 \; q_i \; + \; \frac{Q_{q_i}}{I_i} \qquad i = 1, 2, 3, ... \quad (5)$$

where ω_{q_i}, I_i and Q_{q_i} are the modal frequency, modal mass and generalized force terms for each mode i. The differentiation ($\ddot{}$) is done with respect to time t. It can be noticed from equation (5) that the elastic damping is assumed negligible and hence is not accounted for. Each mode shape consists of flap, lag and twist mode shape components, w_i, v_i and φ_i respectively. The generalized force Q_{q_i} consists of the four forcing terms described above and can be written as follows:

$$Q_{q_i} = Q_{aero,q_i} + Q_{tdep,q_i} + Q_{pper,q_i} + Q_{nlin,q_i} \quad (6)$$

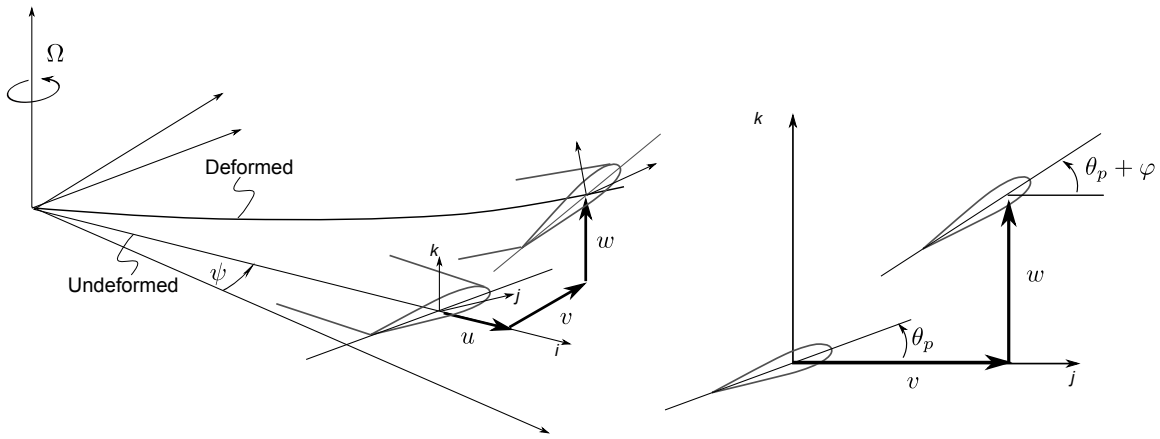

Fig. 1 Schematic diagram for blade coordinate systems and deformation.

where the expressions for the forcing terms can be found in [34]. For the aerodynamic forcing, a blade element technique is used for calculating the forces and moments acting on the blades. Quasi-steady aerodynamic representation [35] is used for calculating the aerodynamic loads at each blade radial station, where the aerodynamic coefficients are interpolated from look-up tables for a range of angle of attack $(-180°, +180°)$ and Mach number. It should be noted that the profile of the aerodynamic coefficients is nonlinear with Mach number and angle of attack in particular beyond the stall condition. Blade/blade and blade/airframe interactions are not considered here.

The blade deformation due to bending and twisting affects the local flow velocities and also angles of attack. In general, the components of the resultant flow velocity at each blade element arise from five sources, namely: blade rotation, free stream due to the helicopter movement, rotor induced velocity, rates of blade bending and rates of change of the pre-deformed blade coordinates. Furthermore, the resultant flow velocity is conventionally resolved into components tangential and normal to the local axes of the blade. The full expressions of these components depend on many variables, including the positions of the blade elements before and after deformation, and can be very long. Hence, they are not presented here but can be found in [34].

The aerodynamic forcing Q_{aero,q_i} in Equation (6) is the most complex term to evaluate in comparison to the rest of the forcing terms. This is due to the complicated nature of the flow field

around the aerofoil section. The general form of Q_{aero,q_i} is given by the integral:

$$Q_{aero,q_i} = \int_0^R \left[\frac{d(L - L_0)}{dr}\ w_i + \frac{d(D + D_0)}{dr}\ v_i + \frac{d(M - M_0)}{dr}\ \varphi_i \right] dr \tag{7}$$

where the three terms on the right hand side represent the force distribution in the flapwise and lagwise direction and the pitching moment distribution respectively. These terms are functions of the flow and blade properties, as well as blade control angles.

The rotor instantaneous thrust T_i can be evaluated simply by summing all elemental vertical forces L and multiplying this by the number of blades N_B. i.e.

$$T_i = N_B \sum_{elem=1}^{N} L \tag{8}$$

where N is the number of blade elements. This value of thrust is only used to estimate the induced velocity within the rotor model. The thrust value used for performance and trimming procedures has to be averaged out across one rotor revolution.

$$T_{av} = \frac{1}{2\pi} \int_0^{2\pi} T_i\ d\psi \tag{9}$$

The inflow is captured via a 3-state Pitt-Peters dynamic wake model [36–38]. This model permits the variations of the induced velocity in both the radial and azimuthal position. Furthermore, it allows the lag dynamics associated with moving a volume of air to be modeled. The inflow model is given for three states as

$$\nu_i\,(r, \psi) = \nu_0 + \frac{r}{R}\,(\nu_s sin(\psi) + \nu_c \cos(\psi)) \tag{10}$$

where ν_i is the induced velocity at an element of radius r and azimuth position ψ. The induced velocity components ν_0, ν_s and ν_c are given in the wind axes by:

$$[\tau] \begin{bmatrix} \dot{\nu}_0 \\ \dot{\nu}_s \\ \dot{\nu}_c \end{bmatrix}_w = - \begin{bmatrix} \nu_0 \\ \nu_s \\ \nu_c \end{bmatrix}_w + [\Lambda] \begin{bmatrix} T_{aero} \\ L_{aero} \\ M_{aero} \end{bmatrix}_w . \tag{11}$$

T_{aero}, L_{aero} and M_{aero} are the thrust and the aerodynamic rolling and pitching moments respectively in the wind axes, and expressions for the matrices $[\tau]$ and $[\Lambda]$ can be found in [36–38].

Finally, the main model equations, which are represented by Equations (2), (5) and (11), can be rearranged in terms of time derivatives of the state vector x to produce the required state-space form:

$$\dot{x} = f(x,p) \qquad \text{where} \qquad x = \{h_s, h_c, \nu_0, \nu_s, \nu_c, q_1, \dot{q}_1, \ldots, q_8, \dot{q}_8\}^T \tag{12}$$

It should be noted that the adopted method of modeling the blade dynamics (modal response equation + blade element method + dynamic inflow model) is widely used in the helicopter industry. Moreover, to further increase the accuracy of the model, the rotor model was constructed in a format that not only allows adding extra states (e.g. blade degrees-of-freedom, inflow states, etc.), but also modeling more complex features of the aerodynamics and/or the rotor structure (e.g. unsteady aerodynamics, dynamic stall, nonlinear modes, etc).

B. Analysis and Results

1. Hover Case

The rotor model was configured to have realistic blade and flight characteristics for a medium sized helicopter (maximum take-off weight around 6.5 tonnes). Continuation runs were first carried out in the hover flight condition over a range of collective pitch angles. The resulting bifurcation diagrams are depicted in Figure 2, for the first lag (q_1) and first flap (q_2) generalized displacements. In the stable hover condition, the blade is in a steady state situation and hence there is no need to use the harmonic oscillator method, since there is no periodic forcing to the system, nor to trim the rotor to certain thrust or flapping angle values.

As θ_{col} is increased from 0°, there is only one stable equilibrium (hover) branch, which becomes unstable between 19.8° and 23°. This equilibrium branch also destabilizes at θ_{col} higher than 27.2°. In the first instability case, the main branch changes stability at two Hopf bifurcation points located at 19.8° and 23°. This type of bifurcation occurs when a complex conjugate pair of eigenvalues crosses the imaginary axis, with non zero imaginary parts. A Hopf bifurcation is also associated with the birth of secondary periodic solutions (Limit Cycle Oscillations 'LCO's'). In Figure 2, both Hopf points are subcritical leading to the birth of unstable periodic solutions, which

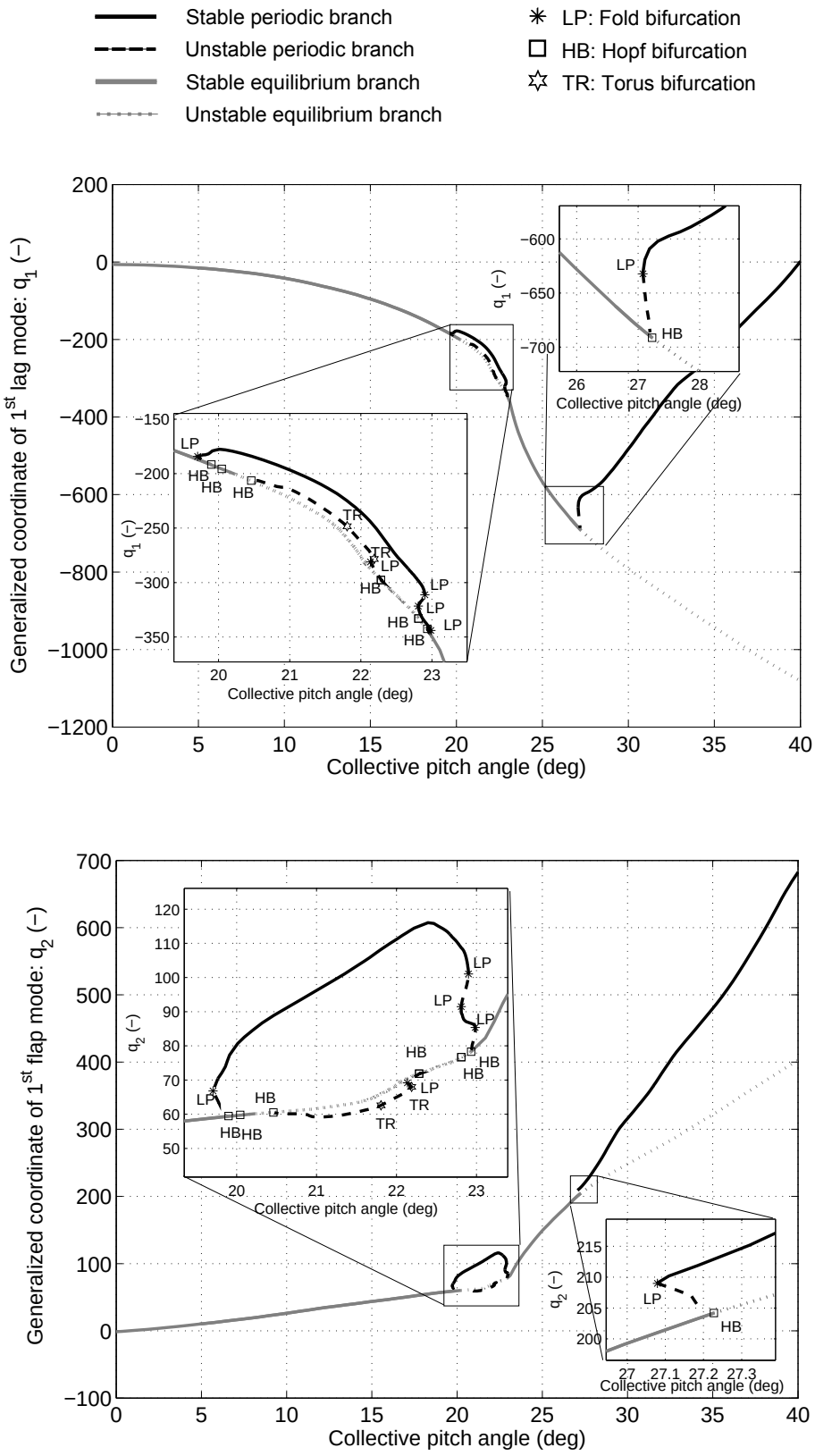

Fig. 2 Bifurcation diagram for hover case using θ_{col} as continuation parameter. Only the peak values of the periodic oscillations in one cycle are plotted.

co-exist with sections of the stable equilibrium branch. A subcritical Hopf is a hard bifurcation which will lead to the solutions jumping to another attractor just after the bifurcation point. This jump can be very dangerous particularly if this latter attractor is far from the original branch. This is because the divergence of the transient oscillatory response, just after the Hopf, can be very rapid and it may not be possible to go back to the stable equilibrium solution, just before the Hopf point, by modest variation of the system parameters, or without significant hysteresis effects. The unstable periodic branch emerging from the Hopf point at $\theta_{col} = 19.8°$ extends very slightly as θ_{col} is reduced and then it folds back at a limit point (fold bifurcation) at $\theta_{col} = 19.6°$. This bifurcation point occurs when one Floquet multiplier crosses the unit circle at a value of 1. The solution then becomes stable and extends as θ_{col} is increased. Furthermore, this stable periodic branch changes stability a few times in the vicinity of $\theta_{col} = 23°$ due to the existence of three other fold bifurcation points, until it merges with the main equilibrium branch at the Hopf point located at $\theta_{col} = 23°$. It can be shown that if the blade is disturbed from the unstable equilibrium branch, it will always get attracted to the stable periodic branch. In other words, if the pitch angle is between 19.8° and 23°, the blade will eventually behave in a periodic manner, i.e. LCO's occur.

The Hopf point at $\theta_{col} = 19.8°$ is found to be associated with the first flap mode becoming unstable, which stabilizes again at $\theta_{col} = 23°$. It was also found that two other flap modes lose and gain stability within the same range of collective pitch angles. This is depicted by four other Hopf bifurcation points within the unstable equilibrium branch. The unstable periodic branch which emerges from two of these points is plotted in Figure 2. This branch also experiences torus (Neimark-Sacker) bifurcations, which will introduce limit cycles of higher period or - more likely - quasi-periodic solutions.

Figure 2 also illustrates the existence of a subcritical Hopf and limit point bifurcation, which fold the secondary unstable periodic branch into a stable periodic one. If the collective pitch angle is increased beyond 27.23°, the solutions will jump to the stable periodic branch. It can also be seen that in the range $\theta_{col} = 27.07°$ to 27.23° the blade can behave either in a stable equilibrium

or in a stable periodic manner, depending on the perturbation levels subjected to the blade.

The maximum operating collective pitch angle for this helicopter is about 12° and hence it is well within the stable region. Although the blade behavior is expected to be stable for this operating helicopter configuration, the above results are useful in supporting the argument that the nonlinear dynamics of the aeroelastic rotating blade does not introduce any secondary branches that extend back to the operating collective pitch range. This is because of the fold bifurcations of the periodic branches that emerged from the subcritical Hopf bifurcation points at $\theta_{col} = 19.8°$ and 27.23°. Additional simulation results confirmed that there are no isolated secondary branches within the operating collective pitch range. Finally, although the bifurcation points occurred well above the 12° limit, this case study provides a good example of how important the construction of the bifurcation diagram is in predicting the global nonlinear dynamics of the blade behavior. In contrast, the traditional stability analysis focuses only on examining the stability of the main branch typically using eigen analysis or Floquet methods, without properly considering the effects of large perturbations. Although, time history simulation can be used to address this shortfall, it is difficult to obtain a clear picture of the underlying structure of the nonlinear dynamics, especially when unstable secondary branches exist in the vicinity of the main solution branch. In additions, for cases where the system is poorly damped, running a large number of time simulations becomes very time expensive.

Finally, for a more complete investigation, the dependence on other parameters would also need to be studied using the continuation and bifurcation analysis. However, for rotor blade aeroelasticity problems, there is at least a moderate number of parameters that can affect the blade stability, for example blade structural and inertial properties, blade control angles and flow parameters. Running the continuation analysis to cover the whole parameter space can be very time expensive or even prohibitive. One solution to this problem is to pick one parameter as the continuation parameter while constraining the others to satisfy a certain condition as the continuation analysis is performed. This method is illustrated in the next section, where the trim condition was selected as a constraint

for the forward flight case.

2. Forward Flight Case

Unlike many analyses, where rotor trimming is carried out first (using the harmonic balance method for example) prior to any stability calculations, some continuation and bifurcation tools such as AUTO can compute solutions and their stability simultaneously for given boundary or integral conditions. This means that the continuation and trimming procedure can be done in parallel. In fact, the eigenvalues and Floquet multipliers are computed at negligible extra cost to the continuation analysis. In addition, the continuation methods used in this work does not require to constrain the periodic solutions to a fixed number of harmonics. Therefore, more accurate solutions as well as trim can be obtained. To achieve rotor thrust and hub moments trim in forward flight, three integral conditions were imposed. The propulsive trim condition to balance the propulsive force with helicopter drag was not explicitly imposed during the continuation. Instead, the rotor shaft inclination was interpolated based on a pre-supplied profile for a range of advance ratio of $0 < \mu < 0.45$. For higher values of μ, the shaft angle was fixed. The boundary conditions can be constructed as follows:

1. The thrust trim condition: in this condition the blade collective pitch angle θ_{col} is obtained by equating the average calculated thrust in one rotor revolution to the required thrust:

$$T_{av} = \frac{1}{2\pi} \int_0^{2\pi} T_i \; d\psi = T_{req} \tag{13}$$

2 & 3. Hub moment or flap angle trim conditions: these conditions allow the determination of the required cyclic pitch angles (A_{lat} and B_{long}) to achieve the desired trim. For flap trim, the first harmonic flap components in longitudinal and lateral directions can be equated to the required values. This can be implemented as follows:

$$\frac{1}{\pi} \int_0^{2\pi} \beta \; \sin(\psi) \; d\psi = \frac{1}{\pi} \int_0^{2\pi} \beta \; h_s \; d\psi = \beta_{a_1,req} \tag{14}$$

$$\frac{1}{\pi} \int_0^{2\pi} \beta \; \cos(\psi) \; d\psi = \frac{1}{\pi} \int_0^{2\pi} \beta \; h_c \; d\psi = \beta_{b_1,req} \tag{15}$$

Figure 3 illustrates the continuation results when the advance ratio is used as the continuation parameter for two rotor disc loading conditions: light and heavy loading conditions. The thrust generated in the heavy loading condition is about 75% more of that in the light weight case. Only the peak values of oscillatory modal displacements of the first two modes are plotted. For the light weight case, the bifurcation diagrams show that when μ is between approximately 1.03 and 1.19 the periodic branch is unstable, due to the presence of two torus bifurcations. Whereas, the instability occurs at a lower value of $\mu \approx 0.82$ for the other case. To further scrutinize the results, the variation of the damping of the modes was investigated from the computed Floquet multipliers. It was found that the unstable periodic branch corresponds to the range of advance ratios when the damping of the first lag mode (mode 1) is negative. Hence, this indicates that this instability can be of the flap-lag type.

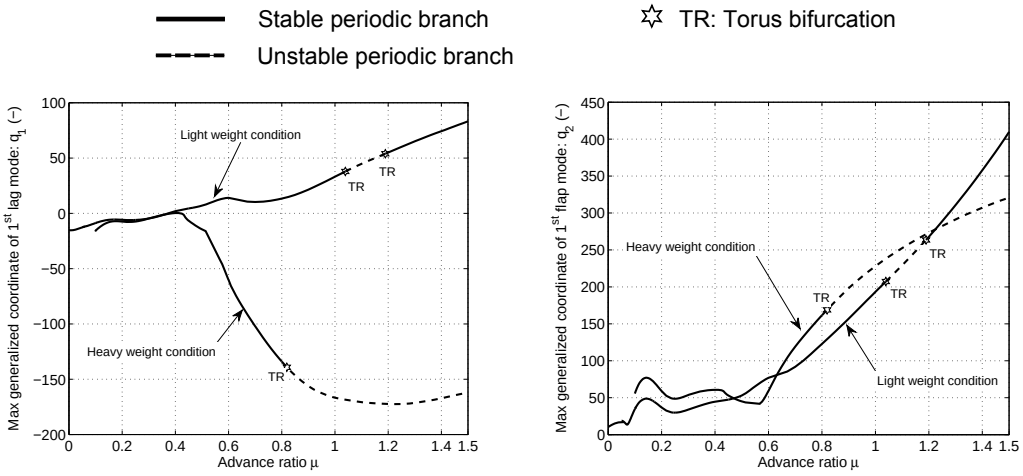

Fig. 3 Bifurcation diagram for forward flight case using μ as continuation parameter. Only the peak values of the oscillations in one cycle are plotted.

It should be noted that although the mathematical model might not be valid for very high advance ratios ($\mu > 0.8$ for example) and the helicopter might not fly at $\mu > 0.55$, it is customary when performing continuation analysis to extend the continuation parameter beyond the physical range. The reason for this is to search for any bifurcation points - especially those subcritical ones - that might lead to new solution branches, which return back into the physical range. Although continuation methods that follow quasi-periodic branches exist, the examination of the

emerging quasi-periodic branches from the torus bifurcations here were done through a series of time simulation runs. For the light weight case depicted in Figure 3, the only secondary branch found was a stable quasi-periodic branch (not shown in Figure 3), which is contained in the range $1.03 \leq \mu \leq 1.19$ and connects the two supercritical torus bifurcations points. Similarly for the second loading case, a stable quasi-periodic branch extends from the torus bifurcation at $\mu \approx 0.82$ with increasing values of advance ratio, most likely to reconnect with another torus bifurcation at $\mu > 1.5$.

Figure 3 illustrates that increasing the rotor disc loading can lead to instability occurring at a lower value of advance ratio. Therefore, it can be argued that for very high loading conditions if the presence of additional sources of nonlinearity causes the torus bifurcations to change their criticality, unstable quasi-periodic branches may extend back to the operating helicopter speed range. Hence, the proper identification of these secondary solutions becomes essential. Finally, although the continuation analysis was not used to follow the secondary quasi-periodic branches, the methods proved very efficient in combining trimmed-flight solutions with the stability analysis and identifying the types of the bifurcation points. Furthermore, the implementation of the harmonic oscillator model for studying rotating blade aeroelastic problems was demonstrated. This technique allows the continuations analysis to follow periodic solutions including those arising from period doubling bifurcations. The implementation of the harmonic oscillator is useful for investigating not only the aeroelastic stability of a passive blade but also when additional forcing is present such as that of an actuated trailing edge flap.

IV. Aeroelastic Stability of Helicopter Rotor Blades with Trailing Edge Flaps

Active Trailing Edge Flaps (TEF) are recognized as effective means for reducing rotor-induced vibrations. However, the interaction between the blade and TEF dynamics might give rise to instability. Furthermore, determining the effects of the activated flap on the blade dynamic characteristics can be a challenging task, in particular with the increased level of nonlinearity of the coupled blade/TEF/actuator/controller system. In this case study, the continuation and bifurcation tools were coupled with an industrial helicopter rotor code to investigate the nonlinear

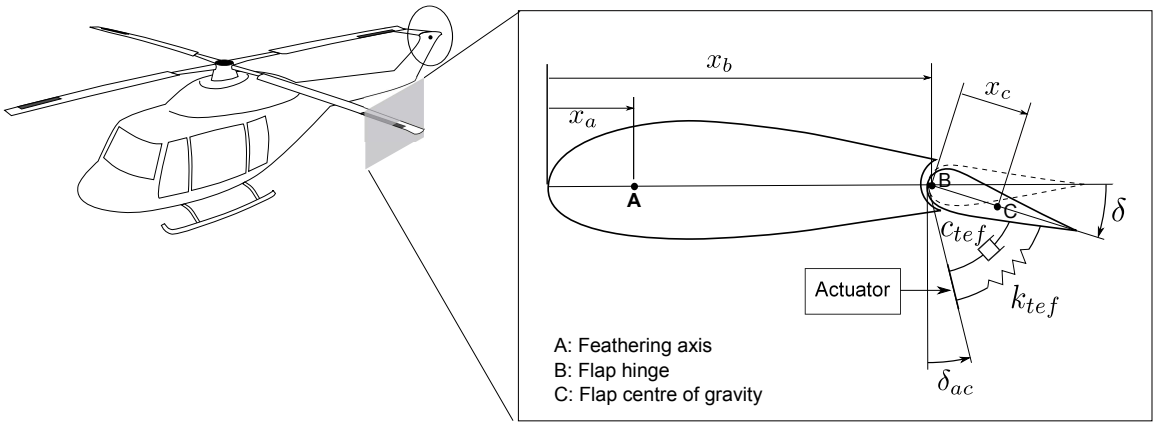

Fig. 4 Schematic diagram of the trailing edge flap.

stability of a passive trailing edge flap incorporated in a flexible rotor blade. The aim is to investigate if the inherent nonlinearity in the blade/TEF system can result in unstable behavior even without including any structural or control nonlinearities to the TEF system. Hence, this study extends the current knowledge on the stability of rotor blade trailing edge flaps to uncover their influence on the coupled blade/flap nonlinear dynamics.

The structure of the rotor model is very similar to that described in Case 1, in that a modal approach is used for describing the dynamics of the flexible blade where each blade is represented by eight general modes (four flap, two lag and two torsional modes). The collective pitch angle was set to an operating hover case value, where the blades' modes are well damped. The TEF was modeled as a rigid control surface hinged at a chordwise distance x_b from the leading edge of the blade, see Figure 4. The structural attachments of the TEF system to the rest of the blade and the driving actuator in the passive mode ($\delta_{ac} = 0$) were represented by a linear rotational stiffness quantity (k_{tef}), which was assumed to act at the flap hinge. The center of gravity (C.G.) of the flap is at distance x_c from the flap hinge. Because of the aerodynamic and inertial couplings between the flap and the blade dynamics the governing differential equations were re-arranged to allow writing them in the state-space form (no acceleration terms on the right-hand-side of the equations).

The parameters of interest in this study are the TEF hinge stiffness and the flap center of

gravity (C.G.) position from the flap hinge. The variation of these two parameters was shown in the literature [27] to affect the linear stability of the flap/blade system and hence bifurcation points can be localized. The flap hinge stiffness represents both the structural spring stiffness at the hinge and the stiffening effects of the TEF actuator components and linkages (in passive mode). The model of the TEF stiffness was purposefully chosen to be linear for two reasons. First, linear (or quasi-linear) stiffness is sufficient to obtain the standard local stability of the main branch. Second, using a linear TEF stiffness allows us to show whether or not the rich TEF dynamics (bifurcations and secondary (periodic) branches) is entirely due to the sources of nonlinearity inherent in the coupled blade/TEF system and not because of the flap stiffness itself. Although, it is not investigated here, it can be argued that additional nonlinearity in the flap stiffness or activating the flap can introduce new bifurcations and/or may change the structure of the secondary solution branches.

Figure 5 presents the bifurcation diagram for the TEF angle δ when the flap C.G. position is used as the continuation parameter. Although the flap chord is only 15% of the total blade chord, the continuation was run up to 50% of the blade chord. This was to search for any bifurcation that may exist outside but close to the physical parameter range. The results show the existence of three bifurcation points: two Hopf bifurcations and one branch point bifurcation. This latter is an indication of a divergence scenario, whereas the Hopf bifurcations are related to flutter or flutter-like instability. It is evident that unstable conditions can arise in the physical limits of C.G. ratio, and that the instability at C.G. ratio of circa 0.22 could potentially give rise to a solution branch that extends back into the physical range.

The location of the bifurcation points will vary with other parameters. A series of continuation runs was therefore performed using the flap C.G. position as the continuation parameter for different hinge stiffness values. The combined bifurcation diagrams were plotted as a projection plot in a two-parameter plane (see Figure 6). This plot illustrates how the flap C.G. position and stiffness parameter plane can be divided into stable and unstable regions, where the bifurcation points trace the stability boundaries. These boundaries can also be computed directly via 2-parameter

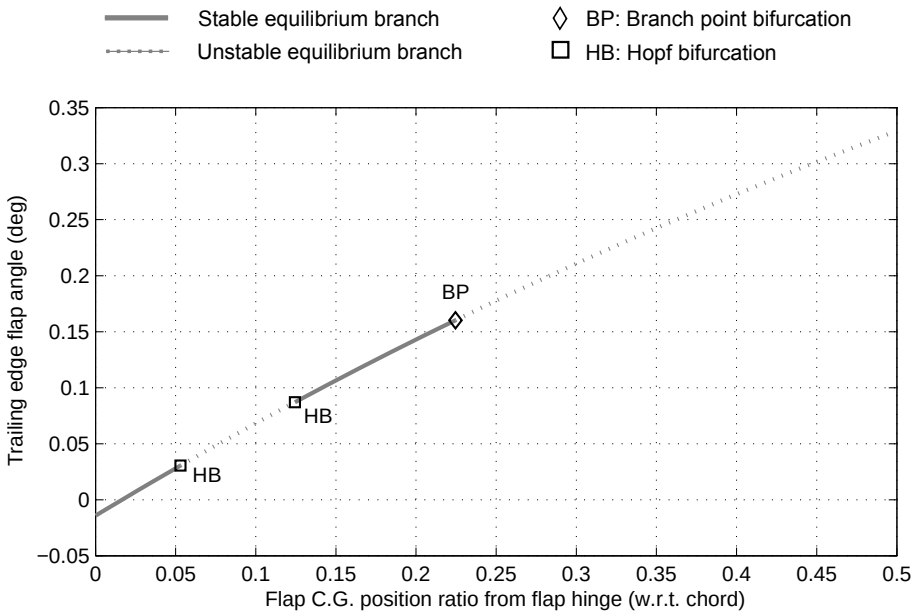

Fig. 5 Bifurcation diagram for an elastic rotor blade with TEF in hover over TEF C.G. position, for flap stiffness of 200 lbs-ft/rad.

continuation runs, where the solutions generated are constrained to match the bifurcation criteria (Hopf or branch point bifurcation in this case). Note that this stability map in parameter space refers to the stability of the main solution surface – as shown in the Figure 5 – and not of any other solution branches arising from bifurcation points. It can be seen that the stable TEF C.G. range decreases for low flap stiffness values. An example scenario where the flap stiffness can be dramatically reduced is the failure case of the TEF actuator (zero stiffness).

Finally, continuation runs were performed to trace the periodic branches emerging from the Hopf bifurcations. Figure 7 illustrates the results of these runs in the form of a more complete bifurcation diagram compared to that of Figure 5. It can be seen that periodic behavior of the flap is quite complex and is subjected to different types of bifurcations, including folds (limit points) and torus bifurcations. There exist a number of stable LCO segments where some of the segments co-exist over the same C.G position range. This means that the flap as well as the blade can oscillate in two or more different forms for the same value of C.G. position, depending only on initial conditions. Furthermore, it can be seen that the periodic branch undergoes a number

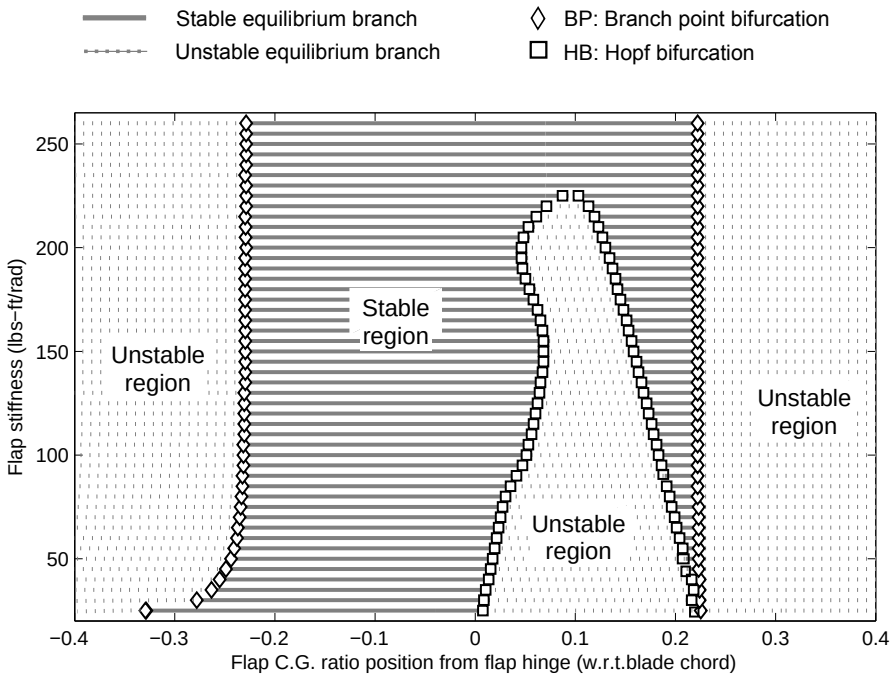

Fig. 6 Stability map in TEF C.G. position and TEF stiffness plane constructed from a series of bifurcation diagrams for an elastic rotor blade with TEF in hover.

of torus bifurcations which will - in turn - lead to the birth of additional quasi-periodic solution branches (not shown here).

The results of Figure 7 illustrate how the fold bifurcations led to the multiplication of the number of different periodic solutions within the same C.G. position range. The case when the solution branch becomes unstable is of great importance, as the unstable branch can be seen as a boundary between two different dynamics (e.g. equilibria and LCO's) in particular, when unstable periodic solutions co-exist with the main stable equilibrium branch. This can be seen in Figure 7 for C.G. position > 0.124 and it can be shown that a moderate disturbance of the trailing edge flap of the order of 2° can lead to unstable behavior even though the main equilibrium branch is stable. Although practically in this case, a small value of C.G. position - residing in the first stable stable range ($< 5\%$) - will be selected in the TEF design, the latter result provides two very important conclusions. First, the nonlinearities (aerodynamic, geometric, inertial, structural) inherent in the blade/TEF system are enough to give rise to unstable flap behavior even when the

main equilibrium branch is stable. Additional nonlinear properties of the TEF system (including the flap, actuator and control law) may lead to a richer bifurcation diagram, with possible secondary unstable branches extending back to small values of flap C.G. positions. Second, the continuation and bifurcation methods are very powerful in uncovering the structure of the TEF dynamics as conventional stability analysis would not provide this information. This is particularly useful when responses under transient conditions are difficult to predict when there are multiple attractors; however, the bifurcation diagrams show clearly where further studies - incorporating time history runs - are needed and, indeed, how to interpret the results thereof.

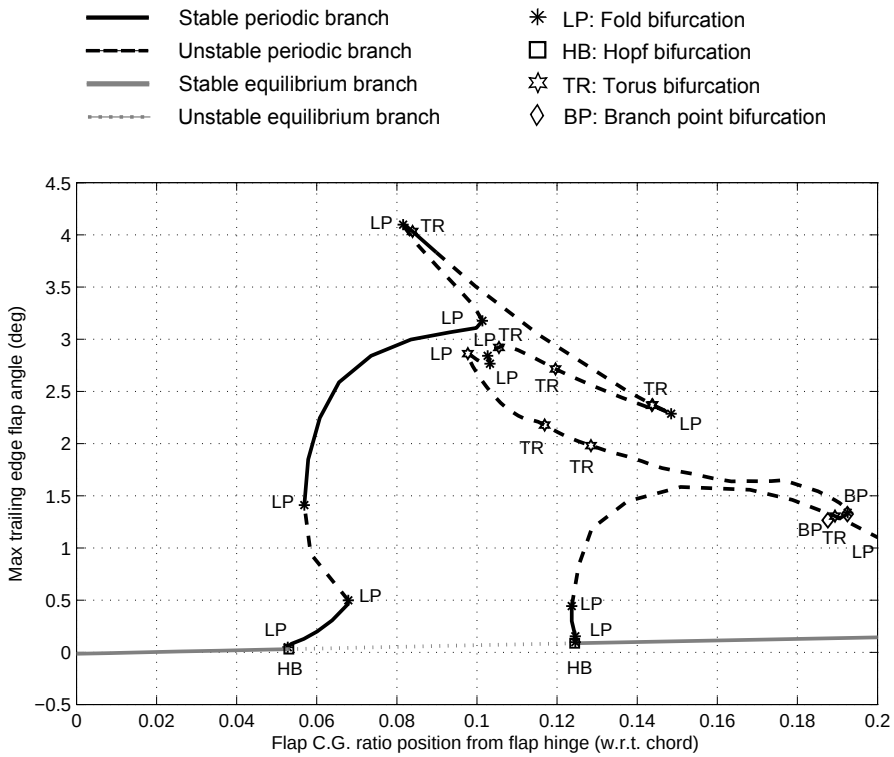

Fig. 7 Bifurcation diagram for an elastic rotor blade with TEF in hover over TEF C.G. position, for flap stiffness of 200 lbs-ft/rad. Only the peak values of the periodic oscillations in one cycle are plotted.

V. Conclusion

This paper presented new implementations of bifurcation and continuation methods in studying the nonlinear helicopter aeroelastic blade stability with and without trailing edge flaps. The aeroelastic model was constructed in a generic state space form. Initially, the analysis was applied to investigate the aeroelastic stability of a flexible rotor blade for a range of collective pitch angles. The results illustrated that even in the hover case the global nonlinear dynamics of the blade are quite complex, giving rise to stable and unstable periodic branches. However, the helicopter configuration used in this case was very stable which resulted in the nonlinear characteristics inherent in the rotating blade to take effect outside the operating collective pitch range. Nevertheless, the results showed how unstable limit cycle branches co-existed with the main stable equilibrium branch. Additional nonlinearities may extend these unstable branches closer to the operating collective pitch angle range. Two forward flight cases were also shown requiring implementation using a harmonic oscillator to impose the necessary periodically forced condition. This exhibited nonlinear behavior beyond the operating envelope of the helicopter, although relatively close to the higher speed regions for the heavy weight case. The efficiency of the technique in combining trimmed-flight solutions with the stability analysis was demonstrated.

The study was then extended to address the nonlinear stability of a passive trailing edge flap incorporated in the elastic blade for the hover case. It was shown that not only were the stability boundaries for the trailing edge flap computed using the continuation techniques, but also secondary stable and unstable periodic branches were followed. The results predicted that unstable periodic branches co-exist with the main stable equilibrium branch for the same values of flap center of gravity position. This meant that large enough disturbances of the trailing edge flap, of the order of 2°, could lead to unstable behavior even though the main equilibrium branch is stable. These results illustrate the advantage of using continuation and bifurcation methods over the conventional stability analysis, which would fail to provide this type of non-local information.

The analysis presented in this paper not only illustrates that continuation and bifurcation

methods are applicable to studying the rotating blade aeroelastic stability, but also confirms that the dynamics of the blade behavior are very complex and nonlinear, even in the hover condition. It was shown that the local linearized analysis is not sufficient to guarantee the stability of the trailing edge flap and large but possible perturbations of the order of 2° can lead to undesirable dynamics. Although most of the complex behavior of the blade was found outside the operational parameter range for this helicopter, the added complexity of future rotor systems including those of the trailing edge systems will introduce different types of nonlinearity that can have adverse stability effects within the operating parameter space and hence need to be treated with care. Finally, the continuation and bifurcation tools were essential in uncovering the global blade dynamics when multiple solutions coexist. Therefore these tools offer considerable advantages in aeroelastic stability analyses of future rotor configurations, in particular where new devices such as active trailing edge flaps, semi-active lag dampers and active pitch-links introduce additional nonlinearities to the system.

VI. Acknowledgment

The authors would like to thank AgustaWestland for funding and supporting of the work presented in this paper.

References

[1] Horvay, G., "Rotor Blade Flapping Motion," *Quart. Appl. Math*, Vol. 5, No. 2, 1947, pp. 149 – 167.

[2] Horvay, G. and Yuan, S. W., "Stability of Rotor Blade Flapping Motion when the Hinges are Tilted: Generalization of the 'Rectangular Ripple' Method of Solution," *Journal of the Aeronautical Sciences*, Vol. 10, 1947, pp. 583 – 593.

[3] Shutler, A. G. and Jones, J. P., "The Stability of Rotor Blade Flapping Motion," Aeronautical Research Council, R & M No. 3178, May 1958.

[4] Wei, F. and Peters, D., "Lag Damping in Autorotation by a Perturbation Method," *Proceedings of the American Helicopter Society 34^{th} Annual Forum*, Washington, D.C., 1978, pp. 78 – 25.

[5] Peters, D. A., "Flap-Lag Stability of Helicopter Rotor Blades in Forward Flight," *Journal of American Helicopter Society*, Vol. 20, No. 4, 1975, pp. 2 – 13,
doi:10.4050/JAHS.20.2.

[6] Lowis, O. J., "The Stability of Rotor Blade Flapping Motion at High Tip Speed Ratios," Aeronautical Research Council, R & M No. 3544, January 1963.

[7] Peters, D. A. and Hohenemser, K., "Application of the Floquet Transition Matrix to Problems of Lifting Rotor Stability," *Journal of American Helicopter Society*, Vol. 16, No. 2, 1971, pp. 25 – 33, doi:10.4050/JAHS.16.25.

[8] Friedmann, P. P. and Hodges, D. H., "Rotary Wing Aeroelasticity - A Historical Perspective," *Journal of Aircraft*, Vol. 40, No. 6, 2003, pp. 1019 – 1046, doi:10.2514/2.7216.

[9] Friedmann, P. P., "Rotary-Wing Aeroelasticity: Current Status and Future Trends," *AIAA Journal*, Vol. 42, No. 10, 2004, pp. 1953 – 1972, doi:10.2514/1.9022.

[10] Kuznetsov, Y., *Elements of Applied Bifurcation Theory*, Springer-Verlag, 1995, chap. 3 - 5.

[11] Sibilski, K., "Bifurcation Analysis of a Helicopter Non-Linear Dynamics," *Archive of Mechanical Engineering*, Vol. 46, No. 2, 1999, pp. 171 – 192.

[12] Sibilski, K., "Nonlinear Flight Mechanics of a Helicopter Analysis by Application of Continuation Methods," *Proceedings of the* 25^{th} *European Rotorcraft Forum,* Rome, Italy, 1999.

[13] Sibilski, K., "A Study of the Flight Dynamics Helicopter Carrying an External Load Using Bifurcation Theory and Continuation Methods," *Journal Of Theoretical And Applied Mechanics*, Vol. 41, No. 4, 2003, pp. 823–852.

[14] Bedford, R. G. and Lowenberg, M. H., "Use of Bifurcation Analysis in the Design and Analysis of Helicopter Flight Control Systems," *Proceedings of the* 29^{th} *European Rotorcraft Forum,* Friedrichshafen, Germany, 2003.

[15] Bedford, R. and Lowenberg, M., "Bifurcation Analysis of Rotorcraft Dynamics with an Underslung Load," *AIAA Atmospheric Flight Mechanics Conference,* Providence, RI, Vol. 1, 2004, pp. 595 – 619, doi:10.2514/6.2004-4947.

[16] Bedford, R. G. and Lowenberg, M. H., "Flight Dynamics Analysis of Periodically Forced Rotorcraft Model," *AIAA Atmospheric Flight Mechanics Conference,* Keystone, CO, Vol. 2, 2006, pp. 1210 – 1228, doi:10.2514/6.2006-6634.

[17] Maradakis, G., *Fundamental Nonlinear Characteristics of Helicopter Flight Mechanics*, M.Phil. Thesis, Department of Applied Mathematics, Glasgow Caledonian University, Glasgow, 2000.

[18] Mokrane, A., *Helicopter Ground Resonance Prediction Using an Integrated Nonlinear Model*, Ph.D. Dissertation, Department of Aerospace Engineering, University of Bristol, Bristol, UK, 2011.

[19] Avanzini, G. and De Matteist, G., "Effects of Nonlinearities on Ground Resonance Instability," *Proceedings of the 34th European Rotorcraft Forum,* Liverpool, UK, Vol. 3, 2008, pp. 2327 – 2378.

[20] Basset, P.-M. and Prasad, J., "Study of the Vortex Ring State using Bifurcation Theory," *Proceedings of the American Helicopter Society 58th Annual Forum,* Montreal, Canada, 2002.

[21] Rezgui, D., Lowenberg, M. H., and Bunniss, P. C., "Experimental and Numerical Analysis of the Stability of an Autogyro Teetering Rotor," *Proceedings of the American Helicopter Society 64th Annual Forum,* Montréal, Canada, 2008.

[22] Rezgui, D., Lowenberg, M. H., and Bunniss, P. C., "A Combined Numerical/Experimental Continuation Approach Applied to Nonlinear Rotor Dynamics," *Progress in Industrial Mathematics at ECMI 2008,* Springer Berlin Heidelberg, Mathematics in Industry, pp. 169–174, 2010, doi:10.1007/978-3-642-12110-4_21.

[23] Lowenberg, M. H., Rezgui, D., and Bunniss, P. C., "Experimental Evaluation of Numerical Continuation and Bifurcation Methods Applied to Autogyro Rotor Blade Aeromechanical Stability," *Proceedings of the ASME 2009 International Design Engineering Technical Conferences & Computers and Information in Engineering Conference,* San Diego, USA, 2009.

[24] Rezgui, D., Lowenberg, M. H., Jones, M., and Monteggia, C., "Application of Continuation and Bifurcation Methods to Aeroelastic Rotor Blade Stability," *Proceedings of 37th European Rotorcraft Forum,* Milan, Italy, 2011.

[25] Roth, D., Enenkl, B., and Dieterich, O., "Active Rotor Control by Flaps for Vibration Reduction - Full Scale Demonstrator and First Flight Test Results," *Proceedings of the 32nd European Rotorcraft Forum,* Maastricht, Netherlands, Vol. 2, 2007, pp. 801 – 814.

[26] Dieterich, O., Enenkl, B., and Roth, D., "Trailing Edge Flaps for Active Rotor Control Aeroelastic Characteristics of the ADASYS Rotor System," *Proceedings of American Helicopter Society 62nd Annual Forum,* Phoenix, AZ, Vol. 2, 2006, pp. 965 – 986.

[27] Shen, J. and Chopra, I., "Aeroelastic Stability of Trailing-Edge Flap Helicopter Rotors," *Journal of the American Helicopter Society,* Vol. 48, No. 4, 2003, pp. 236 – 243, doi:10.4050/JAHS.48.236.

[28] Maurice, J.-B., King, F., Fichter, W., Dieterich, O., and Konstanzer, P., "Floquet Convergence Analysis for Periodic Active Rotor Systems Equipped with Trailing Edge Flaps," *Proceedings of the 35th European Rotorcraft Forum,* Hamburg, Germany, Vol. 2, 2009, pp. 701 – 714.

[29] Straub, F. and Charles, B., "Aeroelastic Analysis of Rotors with Trailing Edge Flaps Using Comprehensive Codes," *Journal of the American Helicopter Society,* Vol. 46, No. 3, 2001, pp. 192 – 199,

doi:10.4050/JAHS.46.192.

[30] Doedel, E. J., Oldeman, B. E., Champneys, A. R., Dercole, F., Fairgrieve, T. F., Kuznetsov, Y. A., Paffenroth, R. C., Sandstede, B., Wang, X. J., and Zhang, C., "AUTO-07P : Continuation and Bifurcation Software for Ordinary Differential Equations," Tech. rep., Concordia University, Montreal, Canada, 2009. Http://indy.cs.concordia.ca/auto/.

[31] Coetzee, E., Krauskopf, B., and Lowenberg, M., "The Dynamical System Toolbox: Integrating AUTO into MATLAB," *The 16^{th} US National Congress of Theoretical and Applied Mechanics*, State College, Pennsylvania, Vol. USNCTAM2010-827, July 2010.

[32] Leishman, J. and Beddoes, T., "A Semi-empirical Model for Dynamic Stall," *Journal of the American Helicopter Society*, Vol. 34, No. 3, 1989, pp. 3 – 17,
doi:10.4050/JAHS.34.3.

[33] Goman, M. and Khrabrov, A., "A State-Space Representation of Aerodynamic Characteristics of an Aircraft at High Angles of Attack," *Journal of Aircraft*, Vol. 31, No. 5, 1994, pp. 1109 – 1115,
doi:10.2514/3.46618.

[34] Chan, W., *A Coupled Rotor-Fuselage Aeroelastic Analysis Using Complex Rotor Modes*, Ph.D. Dissertation, City University, London, 1996.

[35] Bielawa, R. L., *Rotary Wing Structural Dynamics and Aeroelasticity*, AIAA education series, American Institute of Aeronautics and Astronautics, 2006, pp. 343 - 347.

[36] Pitt, D. and Peters, D., "Theoretical Prediction of Dynamic Inflow Derivatives," *Vertica*, Vol. 5, No. 1, 1981, pp. 21 – 34.

[37] Peters, D. A. and HaQuang, N., "Dynamic Inflow for Practical Applications," *Journal of American Helicopter Society*, Vol. 33, No. 4, 1988, pp. 64 – 68,
doi:10.4050/JAHS.33.64.

[38] Gaonkar, G. and Peters, D., "Review of Dynamic Inflow Modelling for Rotorcraft Flight Dynamics," *Vertica*, Vol. 12, No. 3, 1988, pp. 213 – 242.